NAVAL POSTGRADUATE SCHOOL
MONTEREY, CALIFORNIA

THESIS

A PRELIMINARY EXPERIMENTAL STUDY OF THE BEHAVIOR OF LIQUIDS UNDER TENSIONS

by

Sefa Isik

June 1999

Thesis Advisor: Ashok Gopinath

REPORT DOCUMENTATION PAGE

Form Approved OMB No. 0704-0188

1. AGENCY USE ONLY *(Leave blank)*	2. REPORT DATE	3. REPORT TYPE AND DATES COVERED
	June 1999	Master's Thesis

4. TITLE AND SUBTITLE:
A PRELIMINARY EXPERIMENTAL STUDY OF THE BEHAVIOR OF LIQUIDS UNDER TENSIONS

5. FUNDING NUMBERS

6. AUTHOR(S)
Isik, Sefa

7. PERFORMING ORGANIZATION NAME(S) AND ADDRESS(ES)
Naval Postgraduate School
Monterey CA 93943-5000

8. PERFORMING ORGANIZATION REPORT NUMBER

9. SPONSORING/MONITORING AGENCY NAME(S) AND ADDRESS(ES)

10. SPONSORING/MONITORING AGENCY REPORT NUMBER

11. SUPPLEMENTARY NOTES
The views expressed here are those of the authors and do not reflect the official policy or position of the Department of Defense or the U.S. Government.

12a. DISTRIBUTION/AVAILABILITY STATEMENT
Approved for public release; distribution is unlimited.

12b. DISTRIBUTION CODE

13. ABSTRACT ***(maximum 200 words)***

A set of experiments has been performed to study the extensional behavior of a thin layer of liquid (silicone oil), trapped between two smooth plexiglass disks that are pulled apart in a controlled manner. Different values of separation velocities, liquid viscosities, and liquid layer thicknesses were used to obtain a range of capillary numbers, all in the surface tension dominated regime. Force, displacement, and time information have been recorded for each experimental run. Qualitative visual data has also been gathered for the selected runs. From the quantitative data, force-displacement, and stress-strain plots have been generated to analyze the trends in extensional behavior of the thin liquid layers. Visual data were used to observe the competing regimes (viscous regime and surface tension regime) that are taking place in the process of liquid layer separation. This study could offer fundamental insight into the phenomenon of cavitation and its applications, help to better understand the role of thin liquid layers in material deformations.

14. SUBJECT TERMS
Thin Liquid Layers, Capillary Number, Surface Tension, Viscous Fingering

15. NUMBER OF PAGES 66

16. PRICE CODE

17. SECURITY CLASSIFICATION OF REPORT	18. SECURITY CLASSIFICATION OF THIS PAGE	19. SECURITY CLASSIFICATION OF ABSTRACT	20. LIMITATION OF ABSTRACT
Unclassified	Unclassified	Unclassified	UL

Approved for public release; distribution is unlimited

A PRELIMINARY EXPERIMENTAL STUDY OF THE BEHAVIOR OF LIQUIDS UNDER TENSIONS

Sefa Isik
Lieutenant Junior Grade, Turkish Navy
B.S., Turkish Naval Academy, 1993

Submitted in partial fulfillment of the
requirements for the degree of

MASTER OF SCIENCE IN MECHANICAL ENGINEERING

from the

NAVAL POSTGRADUATE SCHOOL
June 1999

Author: _____
Sefa Isik

Approved by: _____
Ashok Gopinath, Thesis Advisor

_____
Terry R. McNelley, Chairman
Department of Mechanical Engineering

ABSTRACT

A set of experiments has been performed to study the extensional behavior of a thin layer of liquid (silicone oil), trapped between two smooth plexiglass disks that are pulled apart in a controlled manner. Different values of separation velocities, liquid viscosities, and liquid layer thicknesses were used to obtain a range of capillary numbers, all in the surface tension dominated regime. Force, displacement, and time information have been recorded for each experimental run. Qualitative visual data has also been gathered for the selected runs. From the quantitative data, force-displacement, and stress-strain plots have been generated to analyze the trends in extensional behavior of the thin liquid layers. Visual data were used to observe the competing regimes (viscous regime and surface tension regime) that are taking place in the process of liquid layer separation. This study could offer fundamental insight into the phenomenon of cavitation and its applications, help to better understand the role of thin liquid layers in material deformations.

TABLE OF CONTENTS

ACKNOWLEDGMENTS

I would like to express my great appreciation to Professor Ashok Gopinath for his support throughout this research. His dedicated guidance has significantly enhanced my education at the Naval Postgraduate School.

I. INTRODUCTION

The ability of liquids to withstand tension was predicted at the beginning of the last century by Laplace in his theory of capillarity, and it has since been the subject of a good deal of investigation, both theoretical and experimental with relevance to a wide range of applications. [Ref.1] Some well known examples are the behavior of liquid layers in thin film lubrication (involving squeeze and shear), cavitation studies as in underwater explosions (involving high strain rate "tension & tearing" of liquid), and surface tension dominated applications such as painting, coating, etc. (involving compression and tension forces). In addition, on a microscopic scale, the role of thin intergranular liquid layers in material deformations (involving compression, shear, tension forces) is another topic of much interest. But in most prior studies dealing with thin liquid layers, the main focus has been on compression and/or shear forces. It is this feature that distinguishes the present study from previous studies in that the goal here is to explore the behavior of a thin liquid layer (silicone oil) subjected to tension with relevance to above applications.

The forces that need to be dealt with in a thin liquid layer are the viscous force, the surface tension force, the inertia force, and the gravitational. In this study the relative importance of these forces can be ordered as follows:

Surface Tension Force >> Viscous Force >> Inertia Force, and

Surface Tension Force >> Viscous Force >> Gravitational Force.

The Capillary number (Ca) which is a measure of the ratio of viscous forces to surface tension forces, was maintained small (10^{-2}–10^{-6}), which means that surface tension effects were expected to be dominant. The combination of variables (liquid

viscosity and separation velocity) were chosen such a way that the Capillary number would be in the above limits. In addition, by keeping the aspect ratio (width/thickness of the layer) large ($D/l_0 >> 1$), the fluid mechanics in the layer was restricted to essentially one-dimensional behavior.

The nature of the work in this study is experimental, in the course of which, both qualitative visual data, and quantitative force displacement data has been gathered. Both forms of data have been used to make some useful deductions of the mechanics of such layers.

II. BACKGROUND

A. SURFACE TENSION:

1. Physics of Surface Tension:

Atoms at a surface or interface are in an environment that is markedly different from the environment of atoms in the bulk of the material. They may be surrounded by fewer neighbors and these neighbors may be more anisotropic than in the bulk. One often encounters three terms in the scientific literature relating to surfaces: (a) the surface tension, (b) the surface energy and (c) the surface stress. All three quantities have units of energy per area (J/m^2) or force per length (N/m). The term surface tension is appropriate when referring to liquids, because liquids cannot support shear stresses and atoms in the liquid can diffuse fast enough to accommodate any changes in the surface area. This is not the case for solid surfaces and solid-solid interfaces, which usually possess elastic stresses up to the melting temperature. Hence, use of the term surface tension is not clear in the case of solids. [Ref.2]

Today we know that the liquid state itself is composed of molecules in motion that are kept relatively close to each other by attractive Van-der Waals forces. However, a principal method of analysis of problems of interfacial effects rests upon the assumption that the liquid can be described by a continuum *mean-field approximation* or *mean molecular field*, wherein it is assumed possible to define an element of the liquid that is small compared to the range of intermolecular force but large enough to contain a sufficient number of molecules. This approximation implies that on average the attractive force on any molecule in the liquid is the same in all directions giving to the liquid its fluid characteristics. [Ref.3]

a. Liquid-Gas Interface

At a liquid-gas interface although the molecules are free to move in the in the liquid, their motion is far more restricted than in a gas where there is a little attraction between the molecules. Therefore the attraction between the liquid molecules will prevail and prevent the liquid molecules from escaping into the gas. As a result, the liquid molecules at the interface are attracted inward and to the side, but there is no outward attraction to balance the pull because there are not many liquid molecules in the gas (except the ones that escaped by vaporizing). So the liquid molecules at the surface are attracted inward and normal to the liquid-gas interface, which is equivalent to the tendency of the surface contract (shrink).

An alternative explanation is that; molecules deep within the liquid repel each other because of their close packing. Molecules at the surface are less dense and attract each other. Since half of their neighbors are missing, the mechanical effect is that the surface is in tension.

This important boundary condition occurring at the interface, involves the *coefficient of surface tension,* σ, defined as the surface energy per unit interfacial area. A cut of length dL made in a surface will expose a tension force σdL normal to the cut and parallel to the surface. If the surface is curved, these surface forces can cause a pressure jump across the surface.

The dimensions of σ are $\{F/L\}$, with SI units of newtons per meter and BG units of pounds-force per foot.

Surface Tension is effected by:

1)The surface tension decreases with increasing liquid temperature; that is

$$\frac{\partial \sigma}{\partial T} < 0 \qquad (2.1)$$

In practice, σ decreases very nearly linearly with increasing temperature. A typical value is about $-0.1 \text{mN m}^{-1} \text{K}^{-1}$.

At temperatures below freezing, the substance will be a solid, so surface tension is a moot point. As the temperature of a liquid is raised, the surface tension decreases because the cohesive forces decreases. Surface tension is zero at a liquid's critical temperature. If the liquid's critical temperature is known, the *Othmer correlation;*

$$\sigma_2 = \sigma_1 \left[\frac{T_c - T_2}{T_c - T_1} \right]^{\frac{11}{9}} \qquad (2.2)$$

can be used to determine the surface tension at one temperature from the surface tension at another temperature.

2) An insoluble adsorbed monolayer at the surface will also lower the surface tension because the adsorbed molecules will tend to "spread" the surface and hence lower the surface tension since it tends to contract the surface. These surface active materials are called *surfactants* and are capable of reducing the surface tension of the liquid by up to five orders of magnitude.

The effect of surface-active materials in altering surface tension is expressed quantitatively through the *Gibbs equation,* which relates the change in surface tension to the concentration of surface-active materials.

Gibbs equation :

$$\Gamma = -\frac{c}{RT}\frac{\partial \sigma}{\partial c} \tag{2.3}$$

where;

Γ is the surface excess concentration (mol m^{-2}) of the adsorbed solute, and

c is the bulk molar concentration.

The Gibbs Equation shows that there is a decrease in surface tension with an increase in concentration of a particular solute that is positively adsorbed at an interface.

b. Liquid-Liquid Interface

The above discussion for a liquid-gas interface is also aplicable to a liquid-liquid interface between two immiscible liquids with an interfacial tension acting at the interface. As before, there is an imbalance of intermolecular forces, although smaller. The magnitude of the interfacial tension usually lies between the surface tension of each liquid.

(1) Young-Laplace Equation:

Because of the existence of surface tension, there will be a tendency to curve the interface, as a consequence of which there must be a pressure difference across the surface with the highest pressure on the concave side. The expression relating this pressure difference to the curvature of the surface is usually referred to as *Young-Laplace equation.*

$$\Delta p = \sigma\left(\frac{1}{R_1} + \frac{1}{R_2}\right) \tag{2.4}$$

where R_1 and R_2 are the principal radii of curvature of the surface along any two orthogonal tangents, and Δp is the difference in fluid pressure across the curved surface. Note that the individual contribution of either R_1 or R_2 to the pressure difference is negative when moving radially outward from the corresponding center of curvature. From this relation, one deduces three special cases for particular shapes.

$$\text{solid liquid cylinder} : \Delta p = p_i - p_e = \sigma/R \tag{2.5}$$

$$\text{solid liquid droplet} : \Delta p = p_i - p_e = 2\sigma/R \tag{2.6}$$

$$\text{thin-walled bubble} : \Delta p = p_i - p_e = 4\sigma/R \tag{2.7}$$

where R is the body radius.

This formula is consistent with the fact that in stable equilibrium the energy of the surface must be a minimum for a given value of bubble or drop volume, and a sphere has the least surface area for a given volume. For general curved surfaces the radius R is frequently taken to be the mean radius of curvature defined as half the sum of the inverse principal radii of curvature. For immiscible liquids σ refers to the interfacial tension. Obviously for a plane interface, where the mean radius tends to infinity, the pressure difference will be zero.

c. Liquid-Solid Interface

The behavior of liquids on solid surfaces is also considerable practical importance. However, the molecules or atoms at a solid surface, unlike those at a liquid surface, are essentially immobile. Therefore, the solid-liquid interface will not have the same behavior as a liquid-liquid interface. For a planar solid-liquid interface liquid molecules could be attracted more strongly to the solid surface than between the liquid molecules themselves, a situation representative of water on very clean glass. In this case

the liquid molecules would be attracted outward to the interface, but the inward attraction to balance the pull would be less, so the liquid molecules would be attracted outward and normal.

It is almost impossible with solid surfaces to obtain a purely planar surface free from inhomogeneities in contrast to a liquid surface, which can be made to have high degree of homogeneity. Solid surfaces will therefore almost always be contaminated by impurities, which can have a marked effect on the surface tension.

(1) The Static Contact Angle

Young (1805) was the first person to derive an expression for the static contact angle θ. Normally when a liquid drop is placed on a plane solid surface, it will be in contact not only with the surface but often with a gas such as air as shown in fi.

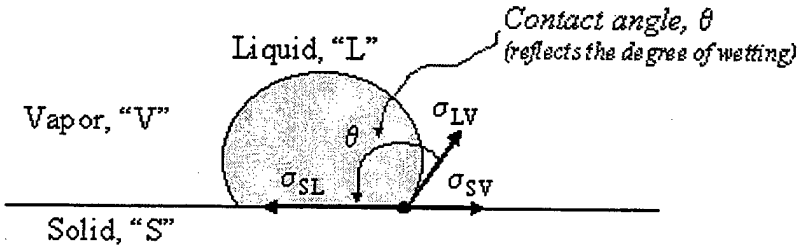

•Young's equation relates interfacial tensions and contact angle

$$\sigma_{SV} = \sigma_{SL} + \sigma_{LV} \cdot \cos\theta$$

Figure 1. Static equilibrium of a liquid drop in a gas at line of contact with a horizontal solid surface.

The liquid may spread freely over the surface, or it may remain as a drop with a specific angle of contact (θ) with the solid surface. The concept of contact angle is closely related to wettability of liquid, interfacial energy and the work of adhesion. The driving force

for formation of an interface between two materials is the decrease in free energy that occurs when intimate contact is established between the two material surfaces. The energy change per unit area ΔG is given by an equation called the Dupre equation

$$\Delta G = \sigma_{LV} + \sigma_{SV} - \sigma_{SL} \tag{2.8}$$

In the studies of adhesion, it is often useful to know the energy required to separate an interface into two original surfaces. In the ideal case where there is no energy dissipation, the reversible work of adhesion W_{ad} defined as the difference in free energy needed to separate the solid-liquid interface to form solid-vapor and liquid-vapor interfaces respectively, is identically equal to ΔG in above equation, thus,

$$W_{ad} = \sigma_{LV} + \sigma_{SV} - \sigma_{SL} \tag{2.9}$$

Equation (2.9) shows that the work of adhesion increases as the interfacial energy decreases. That is more work is required to separate strongly bonded low energy interfaces than weak, high energy ones. Combining Eq. (2.9) with Young's Equation for the contact angle θ then gives

$$W_{ad} = \sigma_{LV}(1 + \cos\theta) \tag{2.10}$$

Equation (2.10) provides a relationship between the work of adhesion and contact angle θ, where we see that W_{ad} is maximum when θ approaches zero and that it also scales with σ_{LV}. [Ref. 2]

2. Capillarity and Capillary Motion

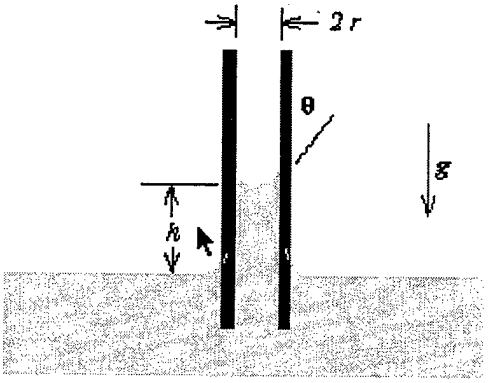

Figure 2. Liquid rise in an open capillary

Capillarity is the phenomenon in which the surface of a liquid is observed to be elevated or depressed where it comes into contact with a solid. For example, the surface of water in a clean drinking glass is seen to be slightly higher at the edges, where it contacts the glass, than in the middle. Capillarity can be explained by considering the effects of two opposing forces: adhesion, the attractive (or repulsive) force between the molecules of the liquid and those of the container, and cohesion, the attractive force between the molecules of the. Adhesion causes water to wet a glass container and thus causes the water's surface to rise near the container's walls. If there were no forces acting in opposition, the water would creep higher and higher on the walls and eventually overflow the container. The forces of cohesion act to minimize the surface area of the liquid; when the cohesive force acting to reduce the surface area becomes equal to the adhesive force acting to increase it (e.g., by pulling water up the walls of a glass), equilibrium is reached and the liquid stops rising where it contacts the solid. In some liquid-solid systems, e.g., mercury and glass or water and polyethylene plastic, the liquid does not wet the solid, and its surface is depressed where it contacts the solid. Capillarity is one of the causes of the upward flow of water in the soil and in plants.

As it was mentioned in the introduction section forces that are needed to dealt with in a thin liquid layer were, surface tension force, viscosity force, gravitational force, and inertia force. The relationship between these forces can be defined in dimensionless parameters. A measure of the hydrostatic gravitational force to surface tension force is given by the Bond number

$$Bo = \frac{gravitational force}{surface tension force} = \frac{\rho g L^2}{\sigma} \tag{2.11}$$

where L is the characteristic length scale. When the Bond number is large, the capillary pressure effect can usually be neglected in a liquid at rest.

A second dimensionless quantity is the Capillary number (Ca) which measures the ratio of the viscous force to surface tension force and is defined by

$$Ca = \frac{\text{viscous force}}{\text{surface tension force}} = \frac{\mu U}{\sigma} \tag{2.12}$$

The ratio of the capillary number to the Bond number is termed the Stokes number. It is a measure of the viscous force to gravity force and is defined by

$$N_{St} = \frac{\text{viscous force}}{\text{gravitational force}} = \frac{\mu U}{\rho g L^2} \tag{2.13}$$

B. LIQUIDS UNDER TENSION

Liquids can under certain conditions sustain quite large tensions. Bertholt tube method was the first method that was tried to measure the amount of tension that water can sustain. A Berthold tube is a sealed tube roughly cylindrical in shape and almost

completely filled with liquid at room temperature and remaining volume being occupied by air and liquid vapor. [Ref. 5] If the tube and liquid is heated until a certain temperature, liquid fills the tube completely, then when it is cooled, the liquid adheres to the walls of the tube until it eventually ruptures. At this point a sudden release of tension is accompanied by a sudden increase in external volume (ΔV) of the Berthold tube; if ΔV can be measured then the critical tension just before the rupture can be determined. In his original work Berthold found that the tension in the water at this instant was 50 atm. Later Temperley and Chambers (1946) found the same tension as 30-50 atm. Rees and Trevena did the same experiment with water in steel tube (1964) and they obtained the values of 10 – 30 atm. [Ref. 1] This results revealed that the nature of walls of the containing vessel in contact with the liquid is important. It was also understood that the previous history of a liquid may alter its properties when subjected to tension. Using of the transducer method by Trevena (1975) allowed it to be monitored not only the rupture tension but also the continuous growth of tension. In 1982 Overton made the same experiments with previously degassed water and evacuated tube in order to remove potential cavitation nuclei in the liquid, and he obtained breaking tensions of up to 68 atm. [Ref. 4] But it is important to note that all these values are not actual tensile strength of the liquid, they represent the weakest link in the liquid container system. Furthermore the values of the critical tension of a liquid under dynamic stressing appear to be consistently less than those obtained under static conditions (e.i. Berthold Tube Method)

C. RECENT STUDIES

In the study of P. McGuiggan, J. Israelachvili, M. Gee, A. Homola, M. Robbins and P. Thompson, the focus was to measure shear forces and other dynamic properties of

liquids in ultrathin liquid films (5-10 A^0) between molecularly smooth mica surfaces. [Ref. 5] Their experimental study showed that, the molecularly thin liquid films between two surfaces depend not only on the types of forces between the liquids and surfaces, but also on the atomic structure of the confining surfaces and how easily the liquid molecules can order relative to the surfaces. Both the static and dynamic properties can be quantized with the number of molecular layers comprising the film, and these properties as well as the number of layers can depend not only on the structure of the liquid and surfaces but also on the externally applied load, the sliding velocity, the direction of the sliding, the elastic properties of the material confining the films, etc. Many of these properties cannot be described, even qualitatively, by conventional parameters, such as viscosity or elasticity modulus, normally applied to bulk liquids or solids.

III. OBJECTIVES OF THE PRESENT STUDY

The objective of the present study is to obtain some fundamental insight into the extensional properties of thin liquid layers subject to tensile forces. Unlike previous studies in this field, the main focus here is on a thin liquid layer (silicone oil) trapped between two smooth plexiglass disks and being pulled apart in a controlled manner in a direction normal to the plane of the liquid layer. There is no shear or compression force involved. The work is experimental in nature and is aimed to gather both qualitative and quantitative data. Experiments have been planned and conducted in a way that some fundamental insights about the effects of initial liquid layer thickness, separation rate and fluid viscosity on force-displacement behavior would be revealed. This study also aims to analyze the different competing regimes in the fluid deformation process.

IV. EXPERIMENT

A. SELECTION OF THE MODEL SYSTEM

There were several concerns in designing the experimental set-up. First of all, since this study essentially deals with thin liquid layers (100-500μm) subjected to only tensile forces, the set-up was designed such a way that it would not allow any undesired forces (shear force etc.) to be involved in the experimental procedure. The actuators (used for positioning and movement) were adjusted to apply only a tensile (pulling force) in the vertical direction, and the stage that holds the circular discs with the trapped liquid layer was aligned perfectly to be perpendicular to the direction of the separation movement of the discs and the plane of the liquid layer. In order to prevent any possibility of introducing tilt or trim to the experiment, the set-up built from heavy materials to provide high rigidity (Figures. 3, 4, 5).

In designing the set-up, it was aimed to have visual data as well as the numerical data. Two CCD cameras were placed in the set-up to provide these data. Since one of the objectives of the experiment was to determine where the separation occurs – whether at the liquid-solid interface or in the bulk of liquid – one CCD camera was placed at the same horizontal level with the liquid film to provide the side view. It was believed that, there would be better understanding of the issue, if another camera recorded spontaneously the movements of the liquid layer from the bottom of the circular discs. Therefore the second CCD camera was placed under the circular discs. This second camera was also fixed to the stage (Figure 3 and Figure 4) to move together with the discs, in order not to lose focus of the liquid film during the motion of the stage. Finally

these two CCD cameras were connected to monitors and the VCRs for viewing and recording (Figure 5).

The experimental set-up was designed to give numerical data from two main sources. First there is the load cell which is connected to an amplifier and multimeter. The load cell was used to gather force and was connected to the computer where these data were stored for further analysis. The second group of data was obtained from the actuators of the positioning system which was controlled by a separate control unit (Figure 6). This control unit was also connected to the same computer to store the data. With a software program, it was also possible to control the actuators by the computer. From the control unit, displacement of the discs and time information, and from the load cell, the force information were recorded. Since the surface area of the solid-liquid interface is another possible important variable in determining the tensile strength of the liquid, disc holders were designed to allow using of different size of discs.

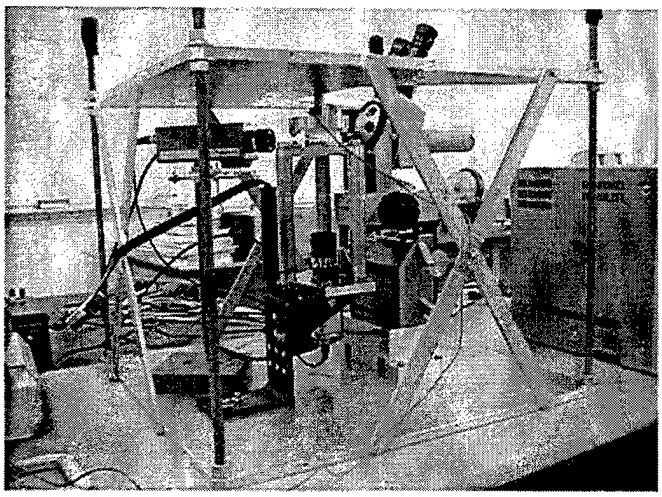

Figure 3. Experimental set-u p

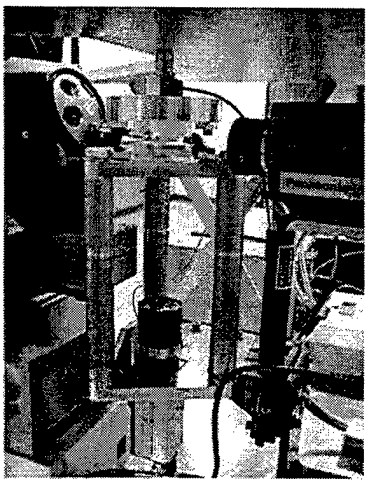

Figure 4. Plexiglass disks, Actuators, Microscope, Side and Bottom CCD Cameras

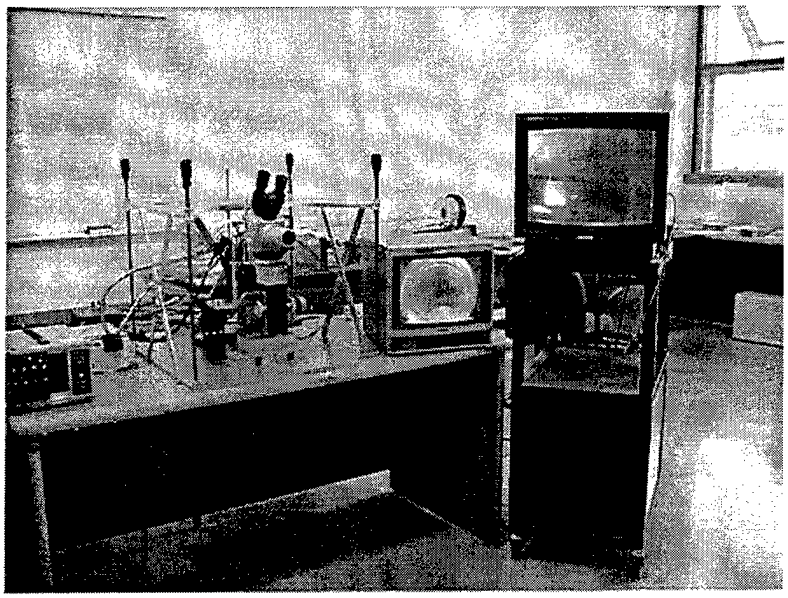

Figure 5. Experimental set-up (monitors for side and bottom views)

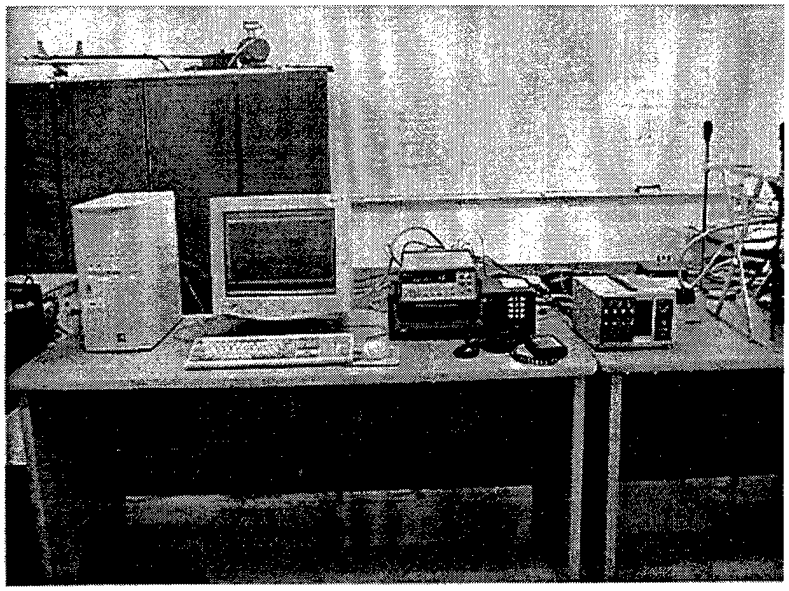

Figure 6. Experimental set-up, (computer, 855C Programmable Controller, Multimeter, Amplifier)

B. EXPERIMENTAL SET-UP

In this section the principal components of the experimental set-up will be introduced in more detailed manner. After designing the model system, the essential components of the system were chosen under the following considerations.

1. Silicone Oil

The "Series 200" range of silicone oils from Dow Corning was found to be the most suitable one for the purposes of this study. They were commercially easy to obtain, and it was possible to obtain these liquids in a range of kinematic viscosities (50 – 100,000 cSt) without any appreciable change in surface tension and density over this entire range. They were also easy and safe to work with, and they had advantageous chemical properties. Detailed information about these liquids is presented in Appendix-A.

2. Positioning System

In the fluid mechanics of thin liquid layers, for surface tension forces to dominate viscous forces the Capillary number (Ca) needs to be small. In order to use silicone oils in small Capillary numbers ($10^{-2} - 10^{-6}$), the required velocities were simply calculated by using (and shown in Figure 7)

$$Ca = \frac{\mu U}{\sigma} \qquad (4.1)$$

Then the positioning system was chosen to provide these desired velocities. The detailed information about the positioning system is presented in Appendix-B.

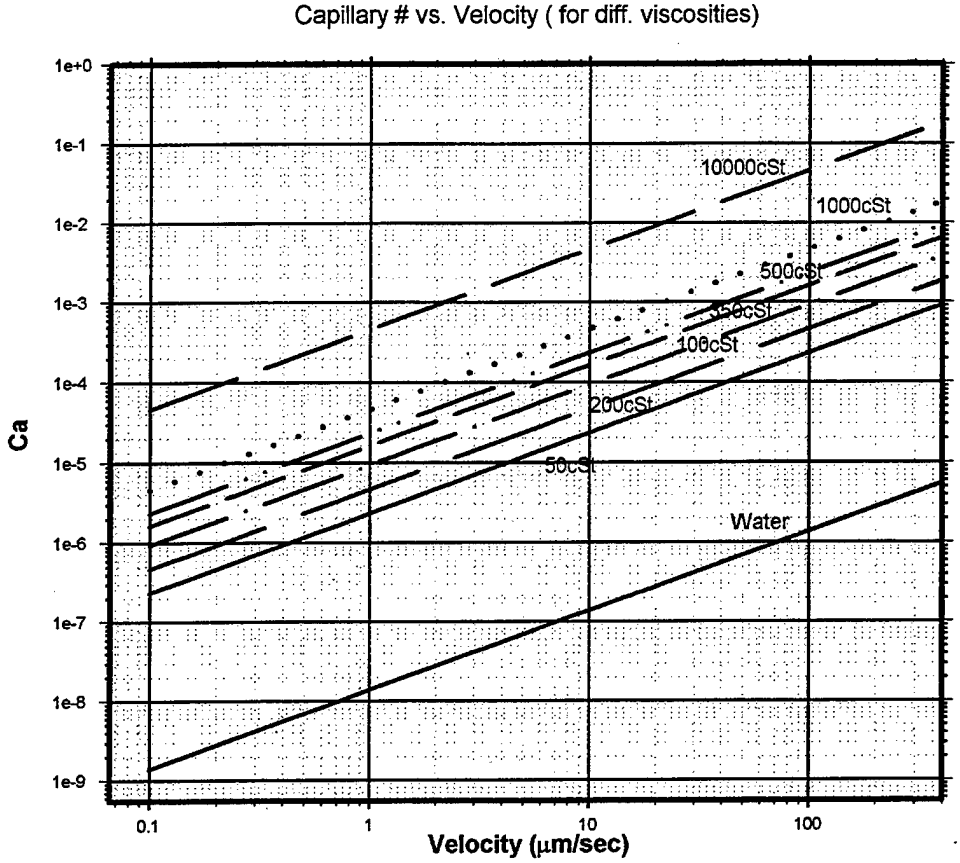

Figure 7. Capillary number vs. Velocity plot

3. Load Cell

Before choosing the load cell, the experiment was conducted in extremely simplified conditions in order to obtain an estimate of the approximate range of forces that the silicone oil might withstand. The results of these experiments were given in Table 1. The other concerns in choosing the load cell were, sensitivity, minimum threshold level, resolution level, possible drifting in measurements with time, signal output, size, accuracy, and ability of being used in tension. The detailed information about the chosen load cell is presented in Appendix-C.

	WATER	SHAMPOO	1000 cSt Silicone Oil	10,000 cSt Silicone Oil
SMALL D=1.5", A=1.76625in^2 W=18gr	0.110 – 0.130 kg	0.090 – 0.100 kg	~ 0.140 kg	0.160 – 0.170
MEDIUM D=2.8", A=6.1544in^2 W=100gr	~ 0.240 kg	0.300 – 0.350 kg	~ 0.300 kg	0.500 – 0.600
LARGE D=4.5", A=15.89625in^2 W=122gr	0.500 – 0.600 kg	~ 0.750 kg	0.600 – 0.700 kg	1.100 – 1.200 kg

Table 1. Results of some preliminary tests

4. Optic Systems

Optic system of the experimental set-up is composed of a microscope that has different magnifying lenses, and two CCD cameras connected to monitors and VCRs. The CCD cameras were positioned so as to get bottom and side views of the liquid layer.

C. EXPERIMENTAL PROCEDURE

Experiments have been conducted in three groups. Each group was named after the liquid that was used. These liquids were 100, 1000, and 10,000 cSt silicone oils. Later the other two variable, initial liquid layer thickness and the separation velocity had been determined. In organizing the groups it was aimed to have at least three different amounts for each variable in order to be able to make a better analysis, and these values were chosen in a way that Ca number would be smaller than 10^{-2}. The variables and the covered ranges are as follows.

LIQUID : Silicone oil, constant surface tension & density
LIQUID VISCOSITY (υ) : 100, 1000, 10,000 cSt
LIQUID LAYER THICKNESS (l_o) : 100, 200, 312, 500 μm
SEPARATION VELOCITY (V) : 1.2 μm/s - 93.7 μm/s
CAPILLARY NUMBER (Ca) : 5.5×10^{-6} - 4.3×10^{-2}

After forming the groups each experiment was conducted according to following procedure.

1) Two plexiglass disks were first separated enough to introduce silicone oil over the lower plexiglass disk.

2) Silicone oil was spread over the lower plexiglass disk through an injector.

3) By commanding the actuator the two plexiglass disks were made to close the gap until the desired layer thickness was achieved. This gap was the initial or starting liquid layer thickness in each experimental run. It was made sure that there was no air bubble in the liquid, and that the liquid had spread completely on both disk surfaces.

4) After the actuator was set to separate at the desired velocity, the computer started recording time, displacement, and force in volts as the load cell output. At the same time views of the both bottom and side cameras were recorded for selected runs.

5) Each run was carried through until complete separation of the liquid film had been achieved.

6) These data have been analyzed by using plots of the force-displacement data and the visual recorded data.

V. RESULTS AND DISCUSSION

In this study experiments have been conducted according to the following combinations of the variables presented in Table 2, 3, and 4.

100 cSt Silicone Oil	**Initial Liquid Layer Thickness (l_o)** 200μm	**Velocity (μm/s)**	48
			24
			12
			4.8
			2.4
			1.2
	Initial Liquid Layer Thickness (l_o) 312.5μm	**Velocity (μm/s)**	48
			24
			12
			4.8
			2.4
			1.2
	Initial Liquid Layer Thickness (l_o) 500μm	**Velocity (μm/s)**	48
			24
			12
			4.8
			2.4
			1.2

Table 2, 3. Experiments conducted with 100 cSt and 1000cSt Silicone Oils

1000 cSt Silicone Oil	**Initial Liquid Layer Thickness (l_o)** 200μm	**Velocity (μm/s)**	48
			24
			12
			4.8
			2.4
			1.2
	Initial Liquid Layer Thickness (l_o) 312.5μm	**Velocity (μm/s)**	48
			24
			12
			4.8
			2.4
			1.2
	Initial Liquid Layer Thickness (l_o) 500μm	**Velocity (μm/s)**	48
			24
			12
			4.8
			2.4
			1.2

10,000 cSt Silicone Oil	**Initial Liquid Layer Thickness (l_o)** 100μm	**Velocity (μm/s)**	48
			24
			12
			4.8
			2.4
	Initial Liquid Layer Thickness (l_o) 200μm	**Velocity (μm/s)**	48
			24
			12
			4.8
			2.4
			1.2
	Initial Liquid Layer Thickness (l_o) 312.5μm	**Velocity (μm/s)**	48
			24
			12
			4.8
			2.4
			1.2
	Initial Liquid Layer Thickness (l_o) 500μm	**Velocity (μm/s)**	48
			24
			12
			4.8
			2.4
			1.2

Table 4. Experiments conducted with 10,000 cSt Silicone Oil.

A. FORCE-DISPLACEMENT PLOTS

All the force-displacement curves show that the force that was needed to separate the liquid layer, increases (almost linearly) until it reaches a peak value (F_{max}) at a location (called d_{max}), after which its value drops down rather suddenly, and drastically, to a value from which there is no significant further change until complete separation.

The values of F_{max} and d_{max} are dependent on the initial liquid layer thickness (lo), the separation velocity (V), the liquid viscosity (υ), and of course surface tension (which was however not varied in the course of this study).

1) Fmax, $d_{max} \propto \upsilon$

For a given initial liquid layer thickness (l_o) and separation velocity, peak force (F_{max}) and the location of the peak force (d_{max}), increase with increasing liquid viscosity (υ) as shown in Figure 8.

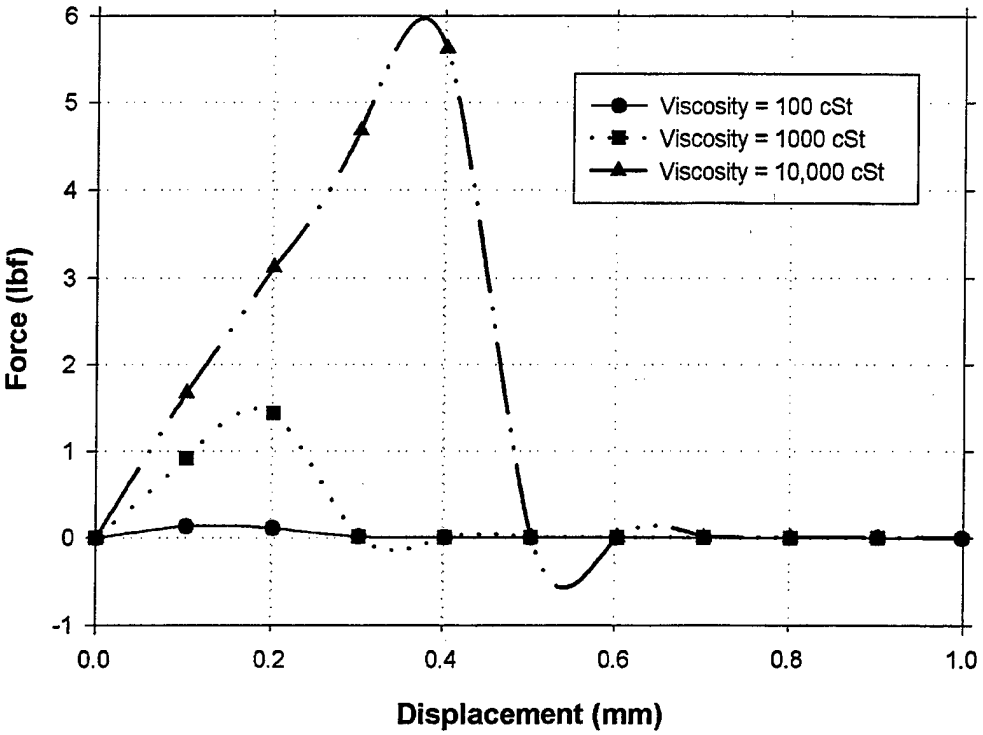

Figure 8. Force-Displacement plot that shows the effect of viscosity on F_{max} and d_{max} Initial Liquid Layer Thickness (l_o) is 200μm, and Separation Velocity (V) is 48μm/s

2) Fmax, $d_{max} \propto V$

For a given liquid viscosity (υ) and initial liquid layer thickness (l_o), peak force (F_{max}) and the location of the peak force (d_{max}), increase with increasing separation velocity (Figure 9).

3) Fmax, $d_{max} \propto 1/l_0$

For a given liquid viscosity (υ) and separation velocity (V), peak force (F_{max}) and the location of the peak force (d_{max}), increase with decreasing initial liquid layer thickness (l_o) (Figure 10).

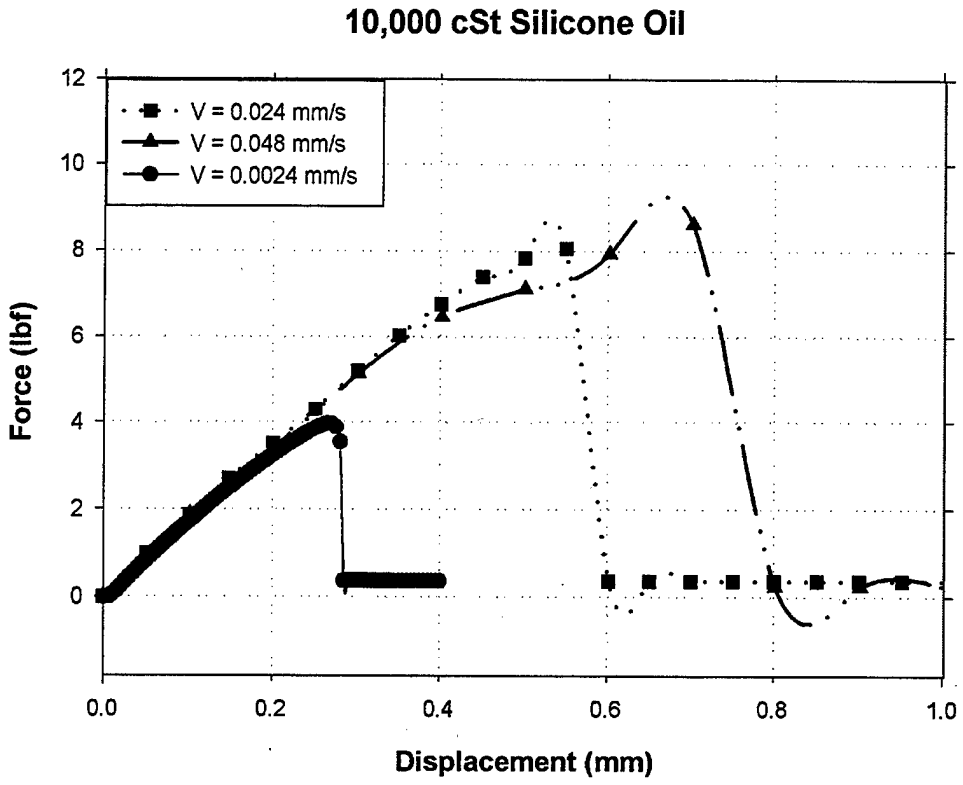

Figure 9. Force-Displacement plot that shows the effect of Separation Velocity on F_{max} and d_{max} Initial Liquid Layer Thickness (l_o) is 100μm

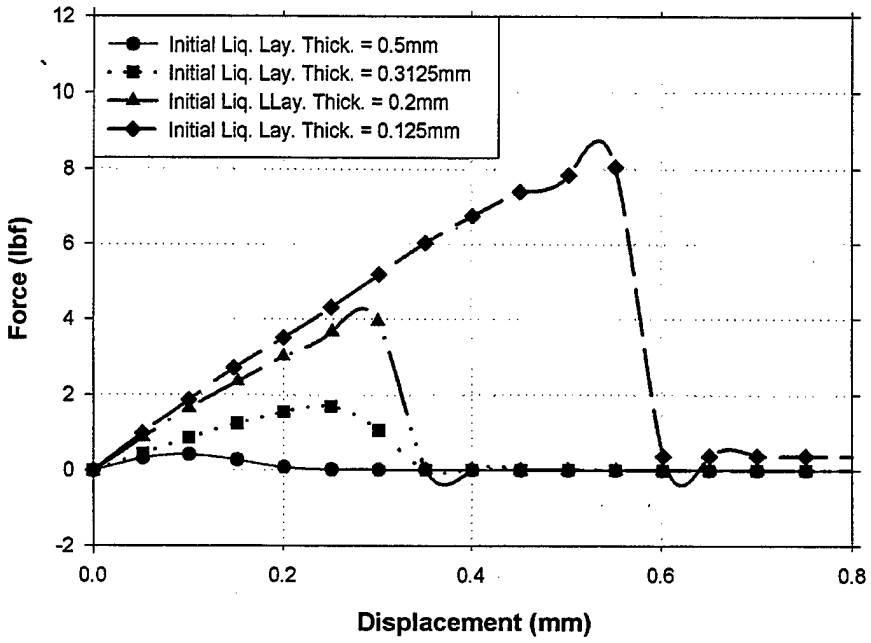

Figure 10. Force-Displacement plot that shows the effect of Initial Liquid Layer Thickness on F_{max} and d_{max} Separation Velocity (V) is 24μm/s and liquid is 10,000 cSt Silicone Oil

4) Stress-Strain Relation

As it can be seen in Figure 11, an initial common linear stress-strain regime was

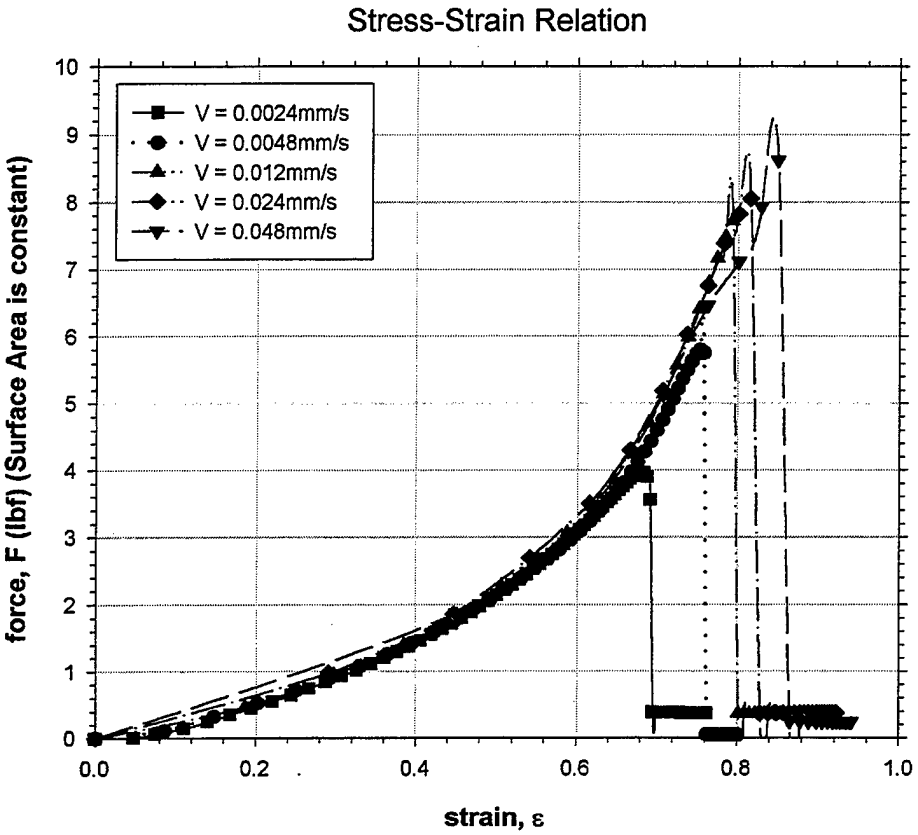

Figure 11. Stress-Strain plot for Initial Liquid Layer Thickness of 100μm and liquid of 10,000 cSt Silicone Oil. For all curves surface area of the disk is constant ($A=\pi(2")^2$)

observed in all the stress-strain curves. A quick calculation using typical bulk modulus values for liquids shows that this behavior is not attributable to any compressibility effects in the liquid. A possible explanation for this behavior could be

due to the restraining surface tension force as the meniscus is stretched. Analysis for a possible mechanism to explain this is presented in Appendix-D.

B. VISCOUS FINGERING

From the analysis of the bottom views, it was understood that during the separation process of the silicone oil there were competing regimes of fluid motion due to

a complicated interplay between viscous and surface tension forces. Figures 12a, b, c, d, 19a, b, c, d present this sequence of events.

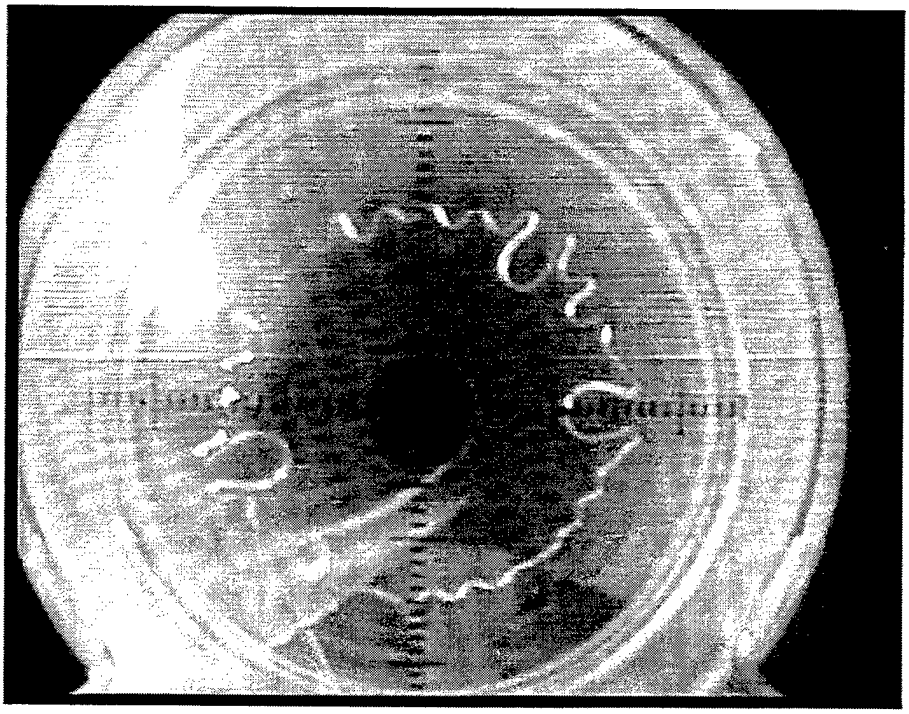

Figure 12a. Onset of viscous fingering effect for 10,000 cSt Silicone Oil which has l_o of 500μm and Separation Velocity of 47μm/s (Scale of 1div=1mm)

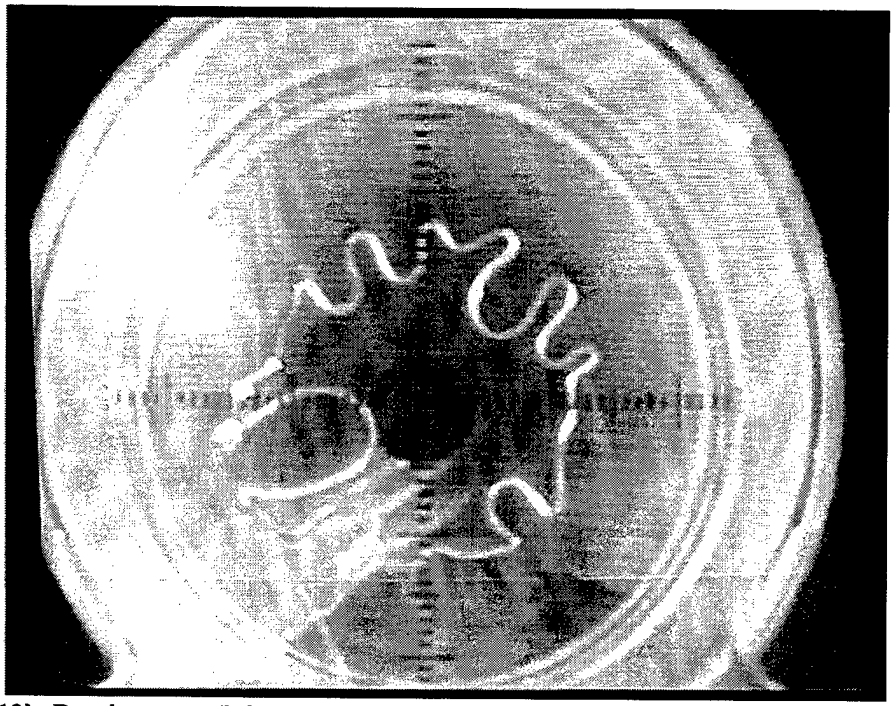

Figure 12b. Development of viscous fingering effect for 10,000 cSt Silicone Oil which has l_o of 500μm and Separation Velocity of 47μm/s (Scale of 1div=1mm)

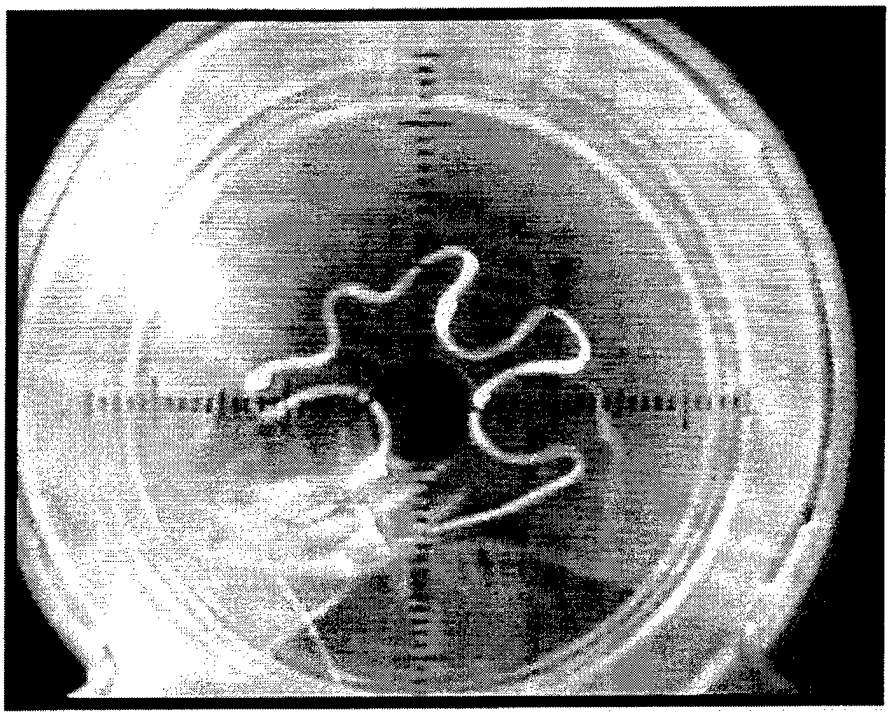

Figure 12c. Progress of the viscous fingering effect for 10,000 cSt Silicone Oil which has l_o of 500μm and Separation Velocity of 47μm/s (Scale of 1div=1mm)

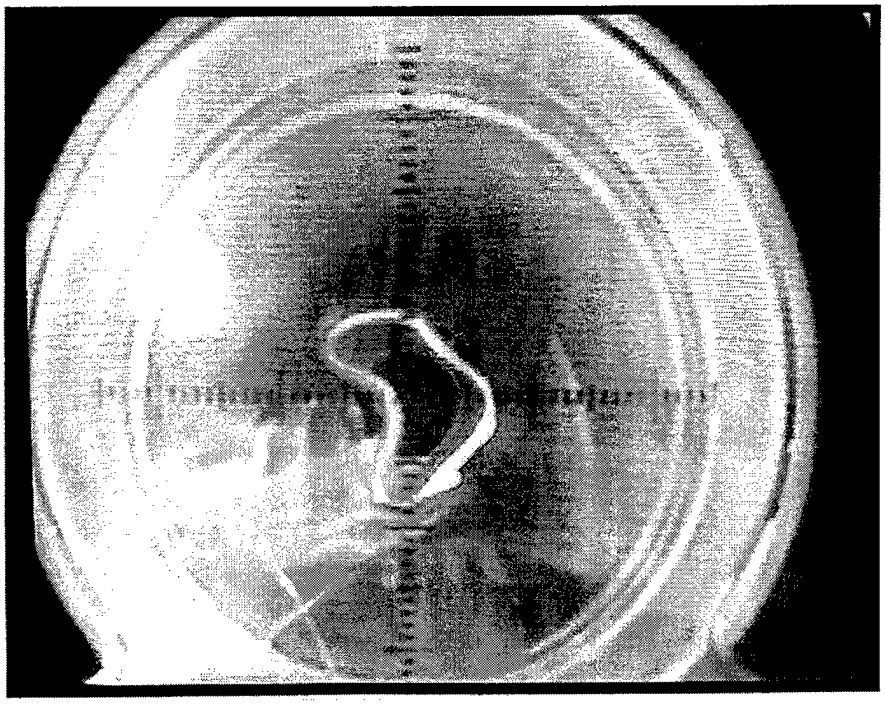

Figure 12d. Final stages of separation for 10,000 cSt Silicone Oil which has l_o of 500μm and Separation Velocity of 47μm/s (Scale of 1div=1mm)

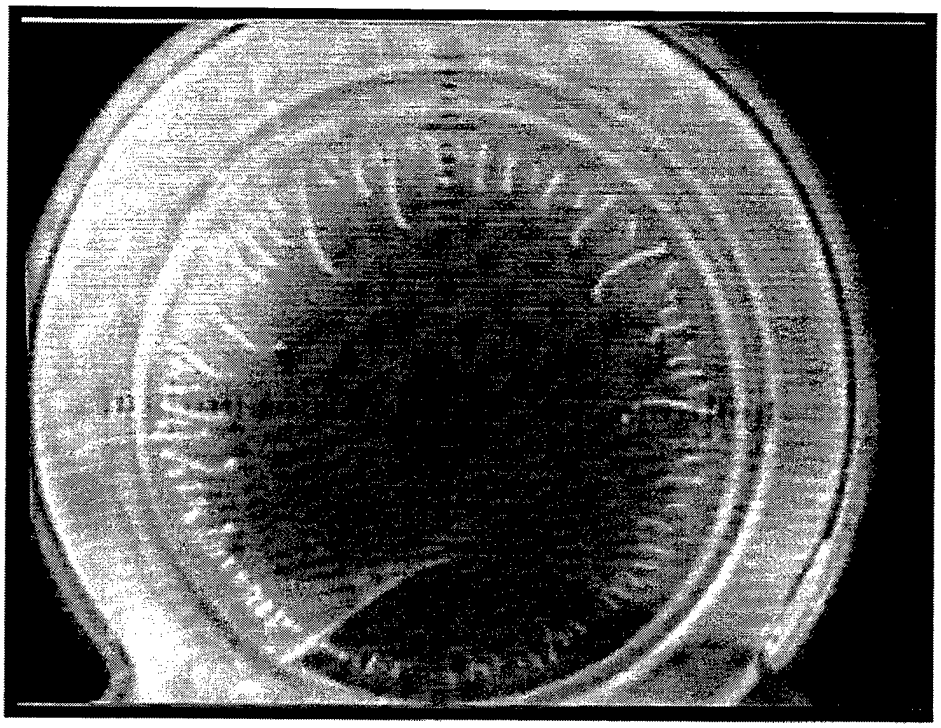

Figure 13a. Onset of viscous fingering effect for 10,000 cSt Silicone Oil which has l_o of 200μm and Separation Velocity of 47μm/s (Scale of 1div=1mm)

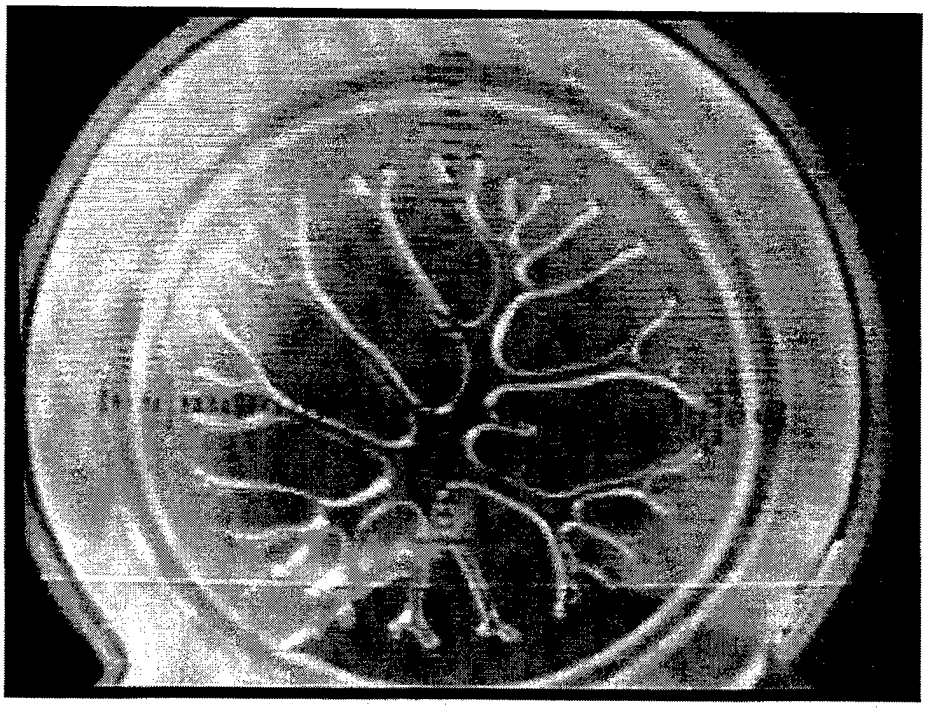

Figure 13b. Development of viscous fingering effect for 10,000 cSt Silicone Oil which has l_o of 200μm and Separation Velocity of 47μm/s (Scale of 1div=1mm)

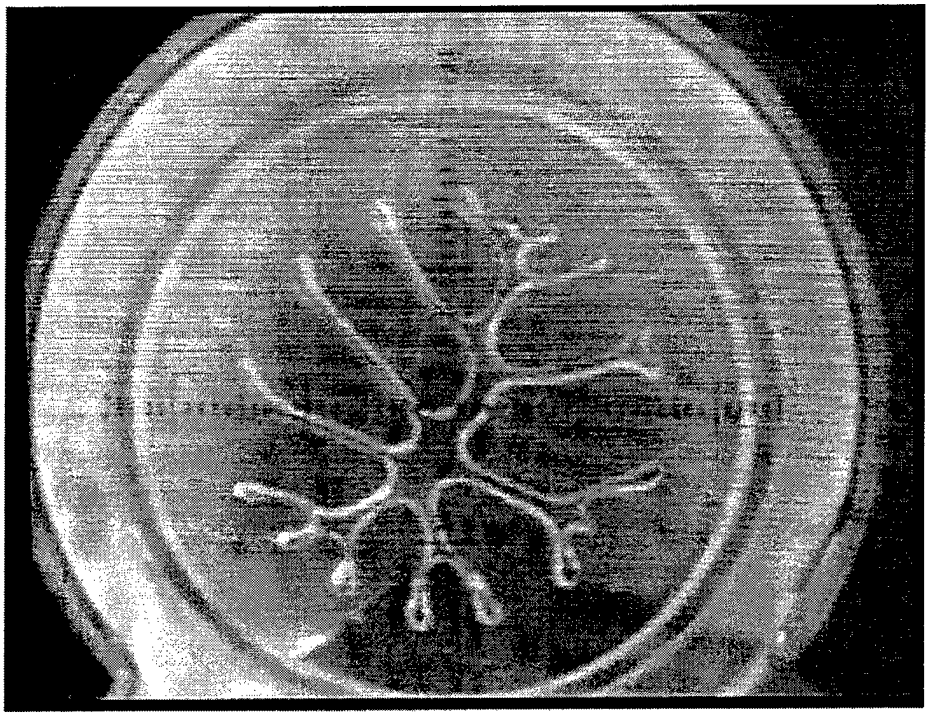

Figure 13c. Progress of viscous fingering effect for 10,000 cSt Silicone Oil which has l_o of 200μm and Separation Velocity of 47μm/s (Scale of 1div=1mm)

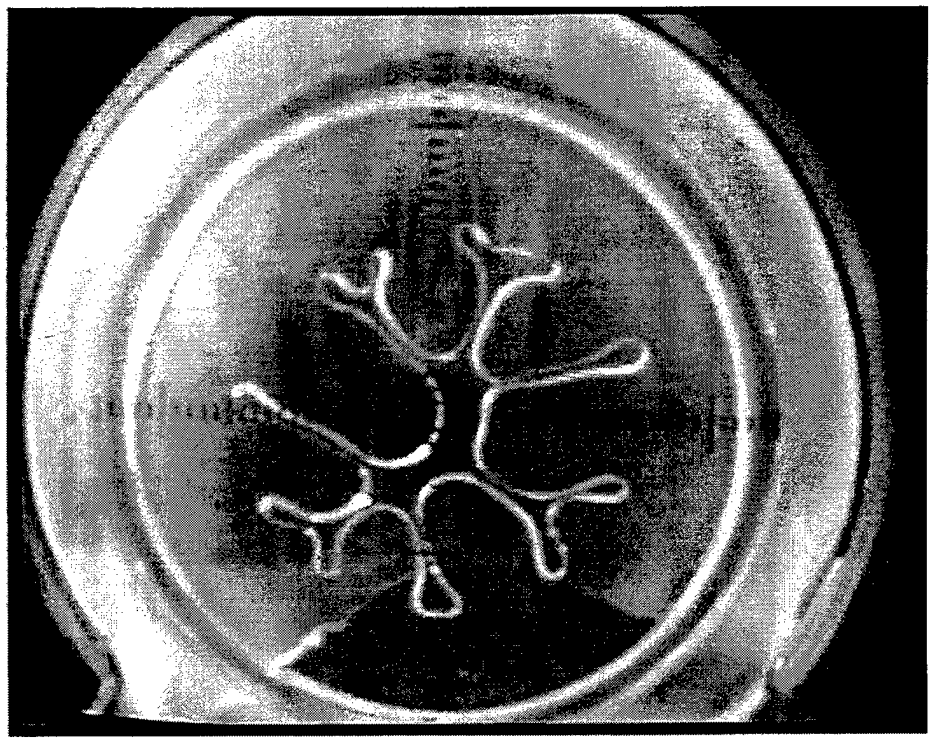

Figure 13d. Development of viscous fingering effect for 10,000 cSt Silicone Oil which has l_o of 200μm and Separation Velocity of 47μm/s (Scale of 1div=1mm)

Viscous fingering can be described as a unique flow process, which is induced by an instability mechanism that occurs when a fluid of higher viscosity is displaced by another fluid of lower viscosity, typically in thin layers and narrow regions [Ref. 6]. The flow is driven by differential pressures imposed at the open boundaries due to the development of this instability. In this process, surface tension provides an important stabilizing effect if the two fluids are immiscible, as it is in this study for the case of the more viscous oil being displaced by the inwardly moving less viscous air. What Figures 12a-13d suggest are, that, at the first moments of the separation process, surface tension force is strong enough to prevent transition and keep the periphery of the liquid layer essentially undistorted and circular. But as the separation process continues, the large difference in viscosities between the oil and the air triggers the instability which is then sufficient to overcome the surface tension force resulting in the viscous fingering.

From the simultaneous comparison of the force-displacement curves, and the video sequences of the separation process, it was clearly revealed that the occurrence of peak force (F_{max}) coincides with the onset of the viscous fingering mechanism.

Comparison of Figure 12a and Figure 13a reveals that the degree of viscous fingering depends on initial liquid layer thickness. As initial liquid layer thickness gets smaller, the viscous fingering effect becomes more pronounced. Similarly, separation velocity (V) and the liquid viscosity (υ) also affect the degree of viscous fingering. Higher the separation velocity and liquid viscosity, greater is the extent of viscous fingering. As a general rule which sums up the combined effect of separation velocity and liquid viscosity, it is more likely to have viscous fingering for high Ca numbers. The

low Ca numbers chosen in the study then assure only an initially surface tension dominated regime.

VI. CONCLUSIONS AND RECOMMENDATIONS

The analysis of the recorded quantitative and qualitative data, clearly shows that there is a certain well-defined trend in the force-displacement behavior of the liquid layers for the chosen configuration of study. All the force-displacement curves have a peak force (F_{max}) whose location and value depend on initial liquid layer thickness, separation velocity, liquid viscosity, and surface tension.

Stress-strain plots define an initially linearly growing stress-strain regime. In this regime surface tension force has a dominant effect and stabilizes viscous force. Approach to the peak force on the force-displacement curve, is accompanied with a subsequent sudden onset of a destabilizing viscous fingering mechanism which leads to a drastic drop in the force. Beyond this point, an essentially flat force-displacement response is observed up to the point of actual "failure".

For further research on this topic it is highly recommended to widen the parametric study to other viscosity and surface tension liquids in order to gather more data to help better understand the mechanisms at play, so as to consequently be able to better predict some of the key quantitative features such as F_{max} & d_{max}. This should also be supported by the development of a better mechanistic model to provide an anlaytical explanation for the different observed regimes.

In addition, varying the disk diameter in order to reveal the effects of contact area, and exploring the role of non-uniform liquid layer thicknesses would be very useful. Using fired (Pyrex) glass instead of plexiglass for the disks would be advantageous to ensure smooth and hard (scratch-resistant) surfaces.

APPENDIX – A

SILICONE OIL

Medium/High Viscosity Silicone Fluids

200® Fluid, 50 cSt
200® Fluid, 100 cSt
200® Fluid, 200 cSt
200® Fluid, 350 cSt
200® Fluid, 500 cSt
200® Fluid, 1000 cSt
200® Fluid, 10,000 cSt
200® Fluid, 12,500 cSt
200® Fluid, 30,000 cSt
200® Fluid, 60,000 cSt
200® Fluid, 100,000 cSt

Description;

200® Fluids from Dow Corning, 50 – 1,000 centistokes (cSt) are medium, and 10,000 – 100,000 centistokes (cSt), are high viscosity polydimethylsiloxane polymers manufactured to yield linear polymers with average kinematic viscosities ranging from 50 – 1000 cSt and 10,000 – 100,000 cSt respectively.

Composition;

Linear polydimethylsiloxane polymers characteristically have the following typical chemical composition:

$$(CH_3)_3SiO[SiO(CH_3)_2]_nSi(CH_3)_3$$

Commercial bulk polymerized dimethl silicone fluids, such as 200 Fluids typically contain trace amounts of process impurities.

Benefits;

200 Fluids, 50 – 100,000 cSt, have the following product charecteristics;

- Clear
- Nongreasy
- Nonocclusive
- Nonstinging on skin

200 Fluids, 50 – 100,000 cSt, when compared with other materials that may be substituted in a given application, may offer one or more of these comparative characteristics;

- High compressibility
- High damping action
- High oxidation resistance
- High shearability without breakdown
- High temperature serviceability
- High compatibility
- High spreadibility
- High water repellency
- Low fire hazard
- Low odor
- Low reactivity
- Low surface energy
- Low temperature serviceability
- Low vapor pressure
- Good heat stability
- Soft feel and lubricity on skin
- Good leveling and easy rubout

APPENDIX – B

POSITIONING SYSTEM

Model 855 Programmable Controller System (Newport Corporation)

The Model 855 Programmable Controller is a microprocessor based system that allows simultaneous direct or programmable control of up to four Newport linear actuators or rotary stages. It is simple but powerful vocabulary of mnemonic commands allows straightforward programming and control via the handheld 855K Keypad/Display or with its standard RS-232C and IEEE-488 interfaces, a remote computer, terminal or modem.

The 855C is compatible with Newport's 850 Series Linear Actuators and Model 496 Power Rotation Stage. Each of these devices use DC motor drives with integral optical encoders for smooth operation and high resolution. The 855C fully supports their resolution and range.

The 855C has four basic operating modes. All are accessible via the 855K Keypad/Display or the RS-232C or IEEE-488 ports. EXECUTE-mode, which the 855C is in at power-up, allows manual precision control of four actuators. From EXECUTE-mode, you may move back and forth between PROGRAM EDIT-Mode, PROGRAM RUN-Mode, and JOG-Mode. PROGRAM EDIT-Mode is for entering, reviewing and editing up to 300 855C instructions into its memory for later, automatic execution in PROGRAM RUN-Mode. JOG-Mode provides a convenient means for repetitively moving actuators back and forth by a specified increment.

The 855C Controller

The 855C Programmable Controller is the nucleus of a system that automatically controls up to four Newport precision positioners and stages. Its large, easy-to-learn instruction set and standard RS-232C and IEEE-488 interface ports allow it to work closely with external computers and other data devices. Its programmability provides stand-alone automatic control of actuator motion, yet no knowledge of programming techniques is required. It also supports the optional 855K handheld Keypad/Display for convenient data entry, control and program editing.

APPENDIX – C

LOAD CELL

ULTRA PRECISION MINI LOAD CELL
UNIVERSAL / TENSION OR COMPRESSION

MDB SERIES

CAPACITY RANGES:
2.5, 5, 10, 25, 50, 75, 100 LBS.

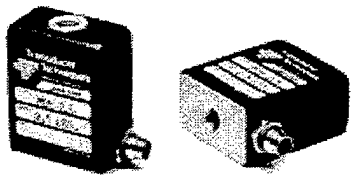

The MDB Series was designed to help fill the growing need for a greater selection of high accuracy load cells for use in space limited applications. The anodized aluminum MDB's are compliant tension and compression, therefore, a good choice for in line through zero applications, as well as single direction tension or compression. Applications may include load feedback for process control, low capacity tensile testing machines, robotics, or designed into your product.

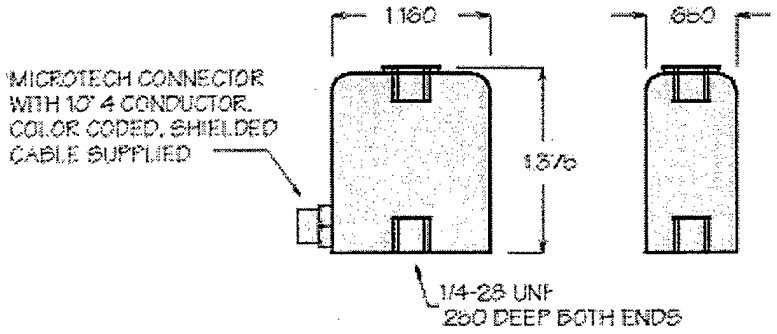

MODEL	CAPACITY LBS.	NATURAL RINGING FREQUENCY HZ	DEFLECTION INCHES
MDB-2.5	2.5	575	.004
MDB-5	5	765	.004
MDB-10	10	1,400	.004
MDB-25	25	2,700	.006
MDB-50	50	3,100	.008
MDB-75	75	3,150	.010
MDB-100	100	3,300	.012

SPECIFICATIONS

Rated Output (R.O.):	2 mV/V nominal
Nonlinearity:	0.05% of R.O.
Hysteresis:	0.05% of R.O.
Nonrepeatability:	0.05% of R.O.
Zero Balance:	1.0% of R.O.
Compensated Temp. Range:	60° to 160°F
Safe Temp. Range:	-65° to 200°F
Temp. Effect on Output:	0.005% of Load/°F
Temp. Effect on Zero:	0.005% of R.O./°F
Terminal Resistance:	350 ohms nominal
Excitation Voltage:	10 VDC
Safe Overload:	150% of R.O.
Weight:	1 oz. all ranges

APPENDIX – D

A SAMPLE CALCULATION FOR THE STRESS-STRAIN CURVE ANALYSIS

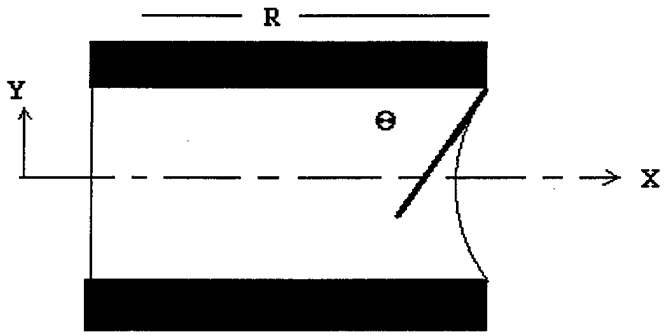

Figure 14. Assumed shape of the liquid layer at the beginning of the experiment (before the separation)

As it can be seen in Figure 14, the disks are aligned such that gravitational force (g), is directed normal to the plane of the liquid layer. If gravitational force "slumping" may be neglected in the gap (Bond number is very small), then the profile of the meniscus may be assumed to be symmetric about the centerplane of the disk.

$$Bo = \frac{\rho g L^2}{\sigma} = \frac{L}{(\Delta_c)^2} \sim \frac{gravitational force}{Surface tension force}$$

where, L: Characteristic Length Scale of the Problem

Δ_c: Capillary Length Scale of the Fluid

For the silicone oils, $\sigma = 21.1$dynes/cm (constant), and $\rho = 0.97$ g/cc

$$\text{Then} \quad \Delta_c \equiv \sqrt{\frac{\sigma}{\rho g}} = \sqrt{\frac{(21.1)}{(0.97)(981)}} \approx 1.5mm = 1500\mu m$$

The gap widths of interest are L_o<300μm (characteristic length scale of the problem)

Note that aspect ratio is $D/L_o \sim 2"/300\mu m > 170$ which for all practical purposes is a one-dimensional problem.

At the start (static) state, for contact angle Θ, we have $\alpha+\Theta = \pi/2$, and the radius of curvature, $r_o = \dfrac{L_o}{2Cos\Theta_c}$ (Figure 15)

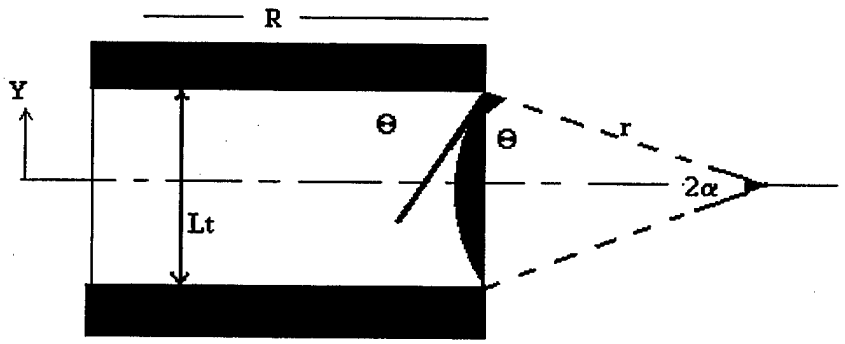

Figure 15. Contact angle

For the shaded (cap area) area in the above figure,

$$r^2\alpha_0 - \frac{1}{2}LrCos\alpha_0$$

$$\left(\frac{L}{2Cos\Theta}\right)^2\alpha_0 - \frac{1}{2}L\frac{L}{2Cos\Theta}Sin\Theta$$

$$\frac{L^2}{4Cos\Theta}\left[\frac{\frac{\pi}{2}-\Theta}{Cos\Theta} - Sin\Theta\right]$$

If $\Theta \sim$ small, $Cos\Theta \to 1$, $Sin\Theta \to 0$

$$A_c \approx \frac{L^2}{4}\left[\frac{\pi}{2} - 2\Theta\right]$$

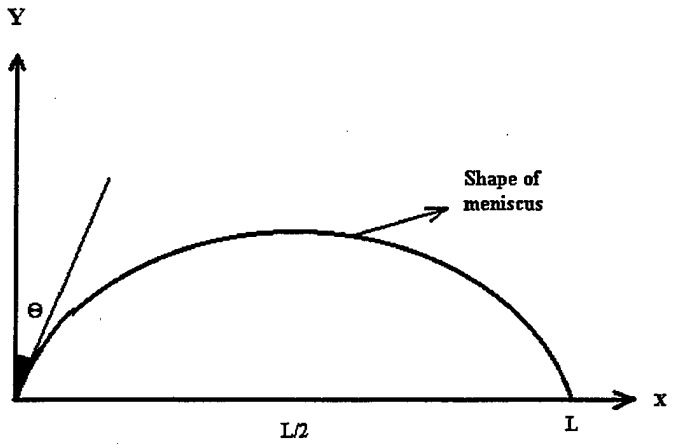

Figure 16. General Polynomial Shape of the meniscus

General Polynomial shape, $f(x) = \sum_{n=0}^{\infty} a_n x^n = a_0 + a_1 x + a_2 x^2 + ...$

Conditions that define the shape of the curve are:

(1) slope due to contact angle, f'(x=0) = Tan(90 - Θ) = Cot Θ

(2) f'(x=L/2) = 0

(3) slope monotonically decreasing, f'(x) < 0

(4) area prescribed

Make use of even function behavior about x = L/2 by shifting the coordinate from

$$x \rightarrow (x - L/2)$$

$$f'(x=0) = Cot\Theta \Rightarrow \left[\sum_{n=1}^{\infty} b_n n (x - L/2)^{n-1}\right]_{x=0} = Cot\Theta$$

$$\Rightarrow b_1 + 2b_2(x - L/2) + 3b_3(x - L/2)^2 + ... = Cot\Theta$$

Applying the above conditions and noting that the meniscus shape be even about x = L/2, only the even powers of (x - L/2) should be retained. This gives,

$$f'(x=0) = Cot\Theta \Rightarrow 2b_2(0 - L/2) = Cot\Theta$$

$$\Rightarrow b_2 = \frac{-1}{L} Cot\Theta < 0$$

So the inverted parabolic shape becomes,

$$f(x) = b_0 + b_2(x - L/2)^2$$
$$f'(x) = 2b_2(x - L/2)$$

where the leading constant is yet to be determined, but is not required to obtain the arc length which is given by,

$$= 2\int_0^{L/2} \sqrt{1 + (f')^2}\, dx$$

Define $$\xi = \frac{2}{L} Cot\Theta (x - L/2) \Rightarrow d\xi = \frac{2}{L} Cot\Theta dx$$

$$arc = 2(\frac{L}{2}\tan\Theta) \int_{-\cot\Theta}^{0} \sqrt{1 + \xi^2}\, d\xi$$

$$arc = \frac{L}{2}\left[\frac{1}{Sin\Theta} Tan\Theta \ln(-Cot\Theta + Csc\Theta)\right]$$

The initial length of the arc based on the initial gap width is,

$$L_0 \frac{(\frac{\pi}{2} - \Theta)}{Cos\Theta}$$

At some intermediate stage of the experiment the arc length is,

$$\frac{L}{2}\left[\frac{1}{Sin\Theta} - Tan\Theta \ln(Csc\Theta - Cot\Theta)\right]$$

The difference in arc length is

$$(L_0 \frac{(\frac{\pi}{2} - \Theta)}{Cos\Theta} - \frac{L}{2}\left[\frac{1}{Sin\Theta} - Tan\Theta \ln(Csc\Theta - Cot\Theta)\right])$$

The difference in arc length above (which is representative of the liquid stretching), can be used along with a knowledge of the contact angle to estimate the force required to overcome the restraining effects of surface tension. However the contact angle for these silicone oils is not known. Visual observations during the course of the experiments suggest that the angle is close to that of water on glass, i.e. a well-wetting

liquid, with angle close to zero. This remains to be verified, but if it were indeed true, then the above difference in arc length could result in large forces. However the slope of the linear portions of the force-displacement curves yield values much larger than those from the above calculations and therefore cannot be explained by surface tension effects alone. A better mechanistic model needs to be developed to provide an analytical explanation for the experimentally observed regimes.

LIST OF FIGURES

LIST OF REFERENCES

1. Trevena, T.H. *The Behavior of Liquids Under Tension*, Contemp. Phys., 1967, Vol. 8, No. 2, 185-195.

2. Howe, James M. *Interfaces in Materials*, John Wiley & Sons, Inc. 1997.

3. Probstein, Ronald F., *Physicochemical Hydrodynamics*, Butterworths, 1989.

4. Trevena, T.H. *Cavitation and the Generation of the Tension in Liquids*, J. Phys. D: Appl. Phys., 17 (1984) 2139-2164.

5. Bratos, S., Hansen, J. P., Leicknam, J. Cl., ed. *Liquid Matter*, Adam Hilger, 1991.

6. Sherman, Frederick S., *Viscous Flow*, McGraw-Hill, Inc., 1990.

INITIAL DISTRIBUTION LIST

No. Copies

1. Defense Technical Information Center.....2
   8725 John J. Kingman Rd., STE 0944
   Ft. Belvoir, VA 22060-6218

2. Dudley Knox Library.....2
   Naval Postgraduate School
   411 Dyer Rd.
   Monterey, CA 93943-5101

3. Chairman, Code ME.....1
   Department of Mechanical Engineering
   Naval Postgraduate School
   Monterey, CA 93943-5000

4. Professor Ashok Gopinath, Code ME/Gk.....2
   Department of Mechanical Engineering
   Naval Postgraduate School
   Monterey, CA 93943-5000

5. Naval/Mechanical Engineering Curricular office, Code 34.....1
   Naval Postgraduate School
   Monterey, CA 93943-5000

6. Deniz Kuvvetleri Komutanligi.....2
   Personel Daire Baskanligi
   Bakanliklar
   Ankara, TURKEY 06100

7. Deniz Harp Okulu Komutanligi.....1
   Kutuphane
   Tuzla, Istanbul, TURKEY 81704

8. Sefa ISIK.....2
   Ordu Cad. Ozturk Apt. No.90 D.5
   Nazilli, Aydin, TURKEY

9. Istanbul Teknik Universitesi Makina Muh. Bl.....1
   Ratip Berber Kutuphanesi
   Maslak, Istanbul, TURKEY